Revista de Metalurgia
April–June 2020, 56(2), e165
ISSN-L: 0034-8570
https://doi.org/10.3989/revmetalm.165

Production of steel 1006 wire reinforced aluminum base composite by explosive welding

Maryam Roudbari, Nima Refahati✉, Ali Mehdipour Omrani

Renewable Energy Research Center, Damavand Branch, Islamic Azad University, Damavand, Iran
✉Corresponding author: nimarefahati@yahoo.com

Submitted: 30 June 2019; Accepted: 20 February 2020; Available On-line: 3 September 2020

ABSTRACT: Aluminum base composites are manufactured in a variety of methods, such as hot rolling, powder metallurgy and explosive welding. The explosive welding is one of the newest methods of Aluminum base composite productions. In this study, aluminum plates were reinforced with steel wires through the explosive welding. Using the numerical simulation and the weldability window of the appropriate parameters were determined. Verification of the results was done using experimental data. Samples were evaluated by a light microscope. The metallography results showed that the composite obtained excellent bonding quality of the interface with no crack. The weldability window and the simulation results agreed very well with the experimental data.

KEYWORDS: Aluminum alloys; AUTODYN; Composite; Steel 1006 wire reinforcement; Weldability

Citation/Citar como: Roudbari, M.; Refahati, N.; Mehdipour Omrani, A. (2020). "Production of steel 1006 wire reinforced aluminum base composite by explosive welding". *Rev. Metal.* 56(2): e165. https://doi.org/10.3989/revmetalm.165

RESUMEN: *Producción de acero 1006 compuesto de base de aluminio reforzado con alambre por soldadura explosiva.* Los compuestos de base de aluminio se fabrican utilizando una variedad de métodos, como laminado en caliente, pulvimetalurgia y soldadura explosiva. La soldadura explosiva es uno de los métodos más nuevos de producción de compuestos de base de aluminio. En este estudio, las placas de aluminio fueron reforzadas con alambres de acero a través de la soldadura explosiva. Utilizando la simulación numérica y la ventana de soldabilidad se determinaron los parámetros apropiados. Los resultados se verificaron utilizando datos experimentales, las muestras se evaluaron con un microscopio óptico. Los estudios de metalografía mostraron que el compuesto que se obtuvo tiene una excelente calidad de unión de la interfaz sin grietas. La ventana de soldabilidad y los resultados de la simulación coincidieron muy bien con los datos experimentales.

PALABRAS CLAVE: Aleaciones de aluminio; AUTODYN; Composite; Refuerzo de alambre de acero 1006; Soldabilidad

ORCID: Maryam Roudbari (https://orcid.org/0000-0002-0433-8485); Nima Refahati (https://orcid.org/0000-0001-8965-3291); Ali Mehdipour Omrani (https://orcid.org/0000-0001-7382-3612)

1. INTRODUCTION

The explosive welding (EXW) technique was used for the first time in World War I (Patterson, 1993). It was at first recognized by Carl in 1944 and then presented into the industry by Philipchuck in 1957 (Honh-bo *et al.*, 2014). The EXW is a solid state process that uses an explosion of explosive material. The flyer plate hits at a specified distance and collides to the base plate (Bataev *et al.*, 2012; Roudbari *et al.*, 2013).

A parallel system in the welding process is shown in Fig. 1. (Gulenc *et al.*, 2016).

The EXW was used to produce multi-layer metals in the form of tubes or plates (Mendes *et al.*, 2013). Moreover, this method was not limited by a variety of metals (Xunzhong *et al.*, 2013). Also in order to manufacture composite reinforced by wire, the EXW were used (Los *et al.*, 2010; Huagui *et al.*, 2017).

The quality of the bonding is dependent on many parameters. The main parameters are the collision velocity, the collision angle, the standoff, etc. (Akbari Mousavi and Al-Hassani, 2008). Due to the fact that the explosive welding is perfected in a very brief time at high temperature and high pressure (Pronichev *et al.*, 2016). So, it is hard to be seen and measured some data directly in a test, and the time history seems hard to realize as well (Los *et al.*, 2010).

Thanks to the advance of software, the finite element method (FEM) has been applied to the study of the EXW (Los *et al.*, 2010). Li *et al.* (2017) studied the numerical simulation of a Titanium/Aluminum laminated composite was manufactured by explosive welding. In a similar work, Aizawa *et al.* (2016) investigated joining Al/Fe using numerical analysis and experimental analysis. Nassiri *et al.* (2015a) predicted the weldability window of parameters by using the finite element simulation. A test was done to verify the simulation and weldability window.

In this study, the optimum operational parameters were predicted to prepare the excellent interface by the weldability window and the numerical analyses. The materials selected for this study were Al1050 and Steel1006. The purpose of this paper is to fabricate Steel wire reinforced Aluminum composite plate with no crack and an acceptable bond.

2. MATERIALS AND METHODS

2.1. Explosive welding model

Numerical simulation of explosive welding was applied by AUTODYN version 14. In this study, Aluminum plates were chosen for the flyer plate and the base plate and the steel wires as reinforcing. A 3D model for the composite set simulation is shown in Fig. 2.

The model has included four materials, such as Aluminum, Steel, Aluminum, and Anfo. The measuring units are used in the AUTODYN, i.e. The length unit is mm, the time unit is ms and the mass unit is mg, the colors of the materials are different in the Autodyne, i.e., the explosive is blue; the flyer plate and the parent are green; the wire is red.

The Johnson-Cook (JC) equation (Nassiri *et al.*, 2015b) was applied for the Al1050 (flyer plate and the parent plate). This equation explains the behavior of material exposed to large deformation (Nassiri *et al.*, 2015b); it can be estimated as follows:

$$Y=\left[A+B\,\varepsilon^{n}\right]\left(1+C\ln\varepsilon^{*}\right)\left[1-\left(T_{H}\right)^{m}\right] \quad (1)$$

with

$$T_{H}=\frac{T-T_{room}}{T_{melt}-T_{room}} \quad (2)$$

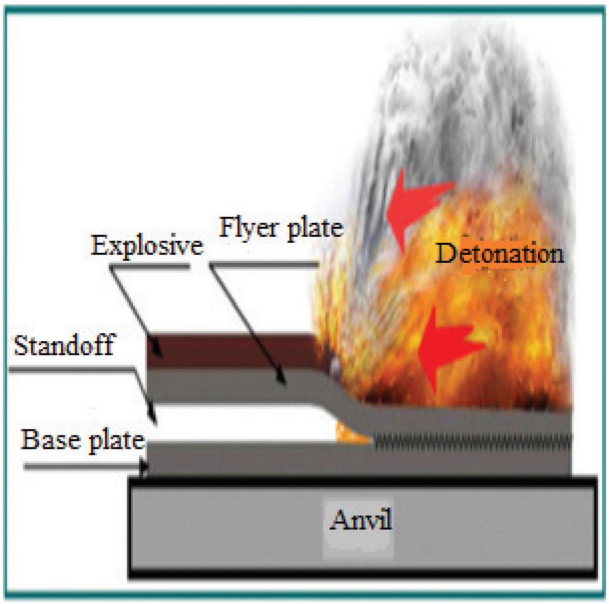

FIGURE 1. A parallel system of the EXW (Nassiri *et al.*, 2015a).

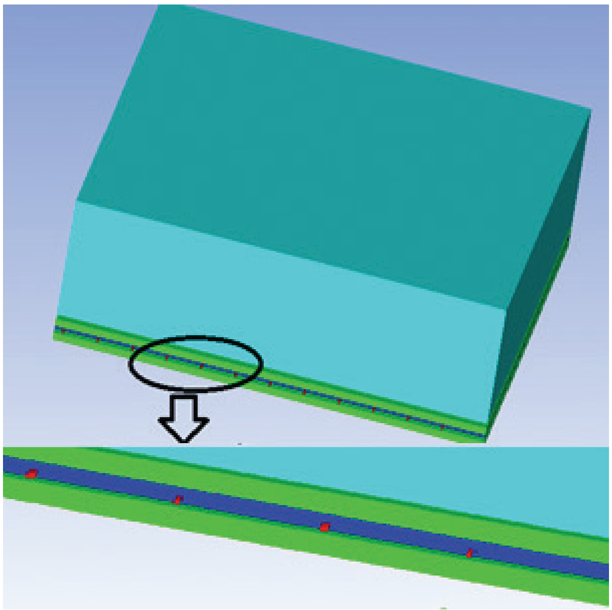

FIGURE 2. The 3D model of the composite set in the AUTODYN.

where Y is the yield stress, ε is the effective plastic strain, ε* is the normalized effective plastic strain rate (often equal to 1), Troom is room temperature, Tmelt shows the melting point of materials and A, B, C, n, and m are the constant equation. The material constants are as listed in Table 1.

The Jones-Wilkins-Lee (JWL) equation of state was applied for the ANFO explosive (Nassiri *et al.*, 2015a). The JWL represents pressure as a subordinate of volumetric strain and special interior energy. The JWL equation is (Los *et al.*, 2010):

$$P = A\left(1-\frac{\omega}{R_1 V}\right)\exp\left(-R_1 V\right) + B\left(1-\frac{\omega}{R_2 V}\right)\exp\left(-R_2 V\right) + \frac{\omega E}{V} \quad (3)$$

where P is the pressure, V represents the relative volume, E is internal energy, w is the Gruneisen parameter, and A, B, R1, R2, are constants of explosive, as shown in Table 2 the default ANFO Constants (Los *et al.*, 2010). The material constants were extracted from the AUTODYN material library.

2.2. Weldability window calculations

There were conditions in the explosive welding that must be met to get proper welds to explain what was named the weldability window/criteria, the weldability zone was developed by Cowan *et al.* (Cowan *et al.*, 1971; Hoseini-Athar and Tolaminejad, 2015). The quality of the connection depends on the EXW welding parameters (Hoseini-Athar and Tolaminejad, 2015), all of the parameters were plotted in the weldability criteria, It could be plotted in both the collision velocity (V_c) and the collision angle (β) (Ribeiro *et al.*, 2014), (Fig. 3). Deribas (1972) and Yingbin *et al.* (2017) suggested the lower limit for the weldability window, which subtended.

$$\beta_{min} = k\left[\frac{H_v}{\rho \cdot V_c^2}\right]^{0.5} \quad (4)$$

where in this Eq. (4) β is in radians, k for high-quality is 0.6 and 1.2 for low-quality and 0.85 for normally-a quality which is a constant, H is the hardness of Vickers for the flyer plate expressed in $N \cdot m^{-2}$ and ρ is the density of the flyer plate in $kg \cdot m^{-3}$ (Hoseini-Athar and Tolaminejad, 2015). Cross land and Bahrani proposed a lower limit of the collision angle is 2°-3° and an upper limit of collision angle is 31° (Zakharenko and Zlobin, 1983).

The upper boundary for the weldability window was reported by Deribas (1972), Wittman (1973) and Zamani and Lighat (2012).

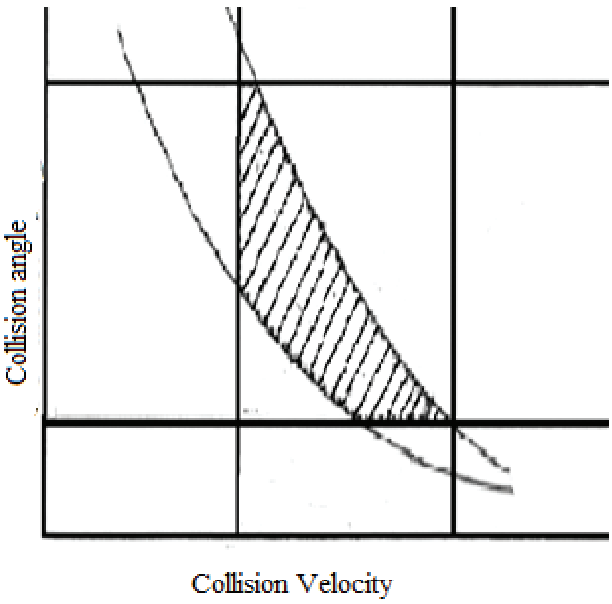

FIGURE 3. Generic weldability window (Nassiri *et al.*, 2015b).

TABLE 1. Mechanical properties of the materials used in this study and their JC parameters (Khanzadeh *et al.*, 2017; Li *et al.*, 2017)

Materials	Density ($kg \cdot m^{-3}$)	Hardness (Hv)	Poisson's ratio	modulus of Elasticity (GPa)	Bulk modulus (GPa)	Melting	A	C	M	N
Steel1006	7896	98	0.29	206	163	1811	350	0.022	1	0.36
Al1050	2710	30	0.33	69	67.4	923.15	110	0.014	1	0.36

TABLE 2. JWL Parameters of the ANFO explosive

Explosive	Detonation velocity ($m \cdot s^{-1}$)	Density ($kg \cdot m^{-3}$)	E ($GJ \cdot m^{-3}$)	A (GPa)	B (GPa)	R1	R2	ω
ANFO	4160	931	2.48	49.46	1.891	3.90	1.11	0.33

$$\sin\left(\frac{\beta}{2}\right)=\frac{k_3}{\left(t^{0.25}\cdot\ V_c^{1.25}\right)} \tag{5}$$

In Eq. (5), β is expressed in radian, t is the thickness of the flyer plate expressed in m, V_c is the collision velocity expressed in m·s^{-1}.

$$k_3=\left[\frac{E}{12\,\rho\,(1-2\,\upsilon)}\right]^{\frac{1}{2}} \tag{6}$$

k_3 is related to the mechanical and physical properties of the Al1050 plates. In Eq. (6), ʋ is Poisson's ratio, E is the elastic modulus in N·mm^{-2} and ρ is the density expressed in kg·m^{-3}.

The left border of the weldability window was linked to the formation of a wavy interface. This limit can be calculated by Eq. (7) (Song *et al.*, 2011).

$$R_e=\frac{\left(\rho_f+\rho_p\right)\,V_c^2}{2\,(H_f+H_p)} \tag{7}$$

Equation (7) in which R_e is equal to 10.6 (Nassiri *et al.*, 2015b), P_f and P_p are the densities of the base plate and flyer plate material in kg·m^{-3}, H_f and H_p are their Vickers hardness and V_c is the collision velocity.

The right border of the weldability window or the maximum collision velocity estimated at 1.2–1.5 times the sound velocity (Yingbin *et al.*, 2017).

2.3. Experimental procedure

In this paper, the test was carried out using the flyer plate (Al1050), the parent plate (Al1050) set up in a parallel formation. For this particular case, the weldability window was plotted. Welding conditions and material properties were selected according to weldability window presented in Tables 1 and 2. In composite plate manufacture, Steel1006 in the diameter of 1 mm was applied as reinforcement. The Aluminum plate of 250×250×4 mm was utilized as a flyer plate, located 4 mm was upper the base plate. The base plate was provided in the size of 250×250×4 mm. The explosive welding was performed using Anfo, the plates and wire mounted in parallel (Fig. 4). The chemical explosive was placed in a box on the flyer plate and the explosion was located on one end of the carton. Moreover, the Steel wire located at zero degree directions relative to the explosion orientation (Fig. 4).

3. RESULTS

The examples of the simulation of the progress of the explosive are shown in Fig. 5–6. Figure 5 shows the position of the base and flyer plates for test 2 ms after detonation. Figure 6 shows the simulation of the test at 4 ms after detonation.

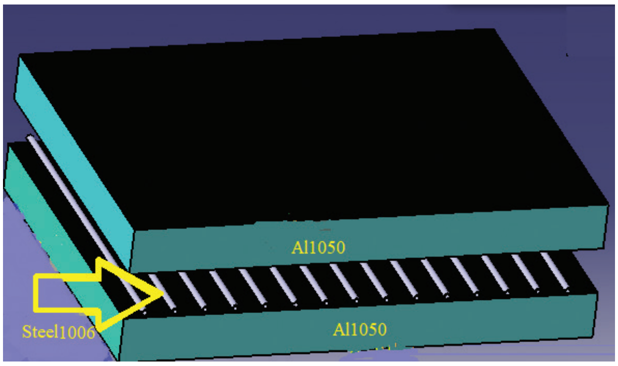

FIGURE 4. The model of Al plates with steel wires (0°).

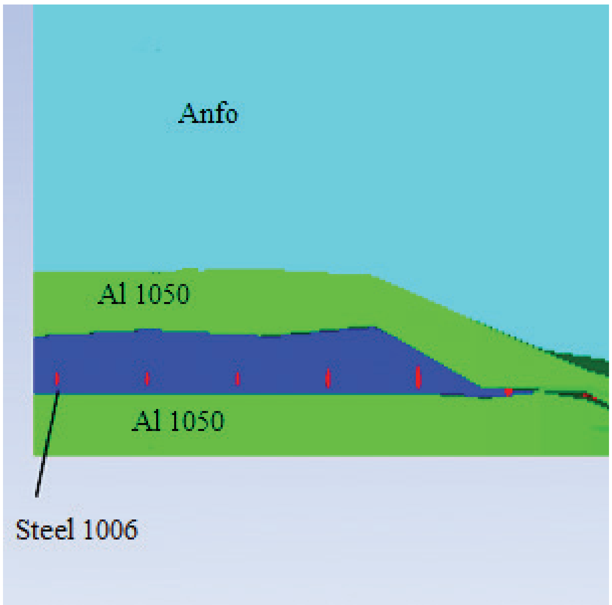

FIGURE 5. Side view of the simulation.

In this paper, the collision velocity (V_c) and the angle velocity (β) were predicated by AUTODYN.

The weldability window is designed based on the collision angle and the collision velocity. Calculated weldability window for the composite set is shown in Fig. 7. The simulation result is placed in the weldability window properly. (Fig. 7)

The interface bonding modality of Al/Steel/Al was examined by the light microscope. Samples of metallographic observations were sectioned from the explosively welded plates. Figure 8 indicates the light microscope images of the bonding interface. It shows that no crack or fault happens at the interface even in the case of magnification of 200 times.

In Fig. 8, the stainless steel wire is located in the middle of the image, which is a circular shape and the Aluminum is surrounded that it is darker than

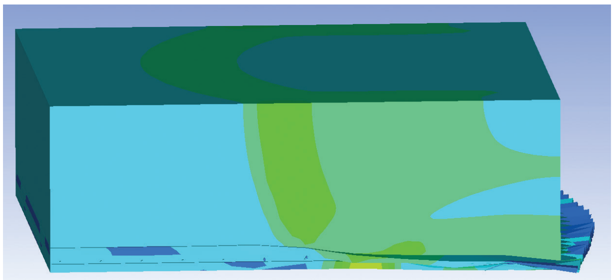

FIGURE 6. Shows the contour of the welding process in 4 ms.

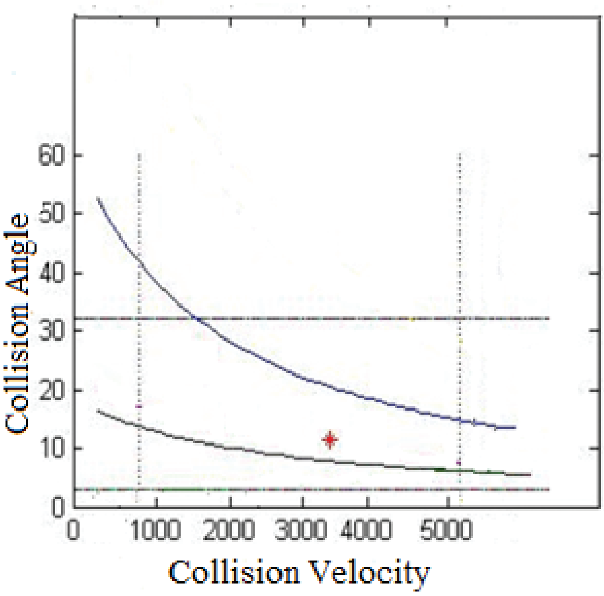

FIGURE 7. The weldability window of Al1050/Al1050.

the wire. It can be observed that the interface of AL/Steel/AL with no void and no macroscope fracture is shown in Fig. 8. The interface showed favorable bonding in the composite plate

4. DISCUSSION

The collision velocity in the simulation was obtained by dividing the length of the material by the total timing of the simulation process was also in agreement with experiments. Moreover, the relationship between the numerical simulation, the weldability window, and the experiment show that all parameters are suitable. The interface bonding is with no void and no crack which shows a good agreement between the finite element results and the experimental data. Gülenc *et al.* (2016) produced stainless steel wire reinforced aluminum composite plate by the explosive welding process, respectively, and their bonding showed no crack or no void.

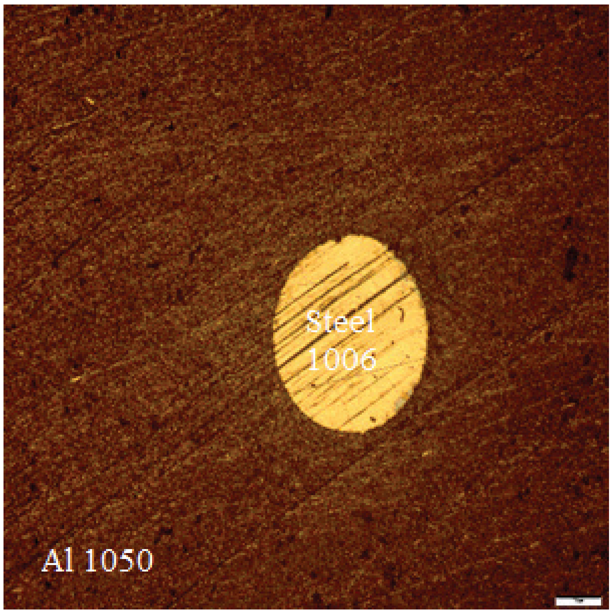

FIGURE 8. The light microscope image of Al/Steel/Al.

All parameters of the composite set predicted by the simulation and the weldability window were agreed very well with the experiment.

5. CONCLUSIONS

In this paper, the weldability window of Al1050/Al1050 was calculated. On this basis, Aluminum base composite reinforced with steel wires were successfully prepared by the explosive welding process and the image of the light microscope with no void was also confirmed the perfect connection Al/steel/Al. The results of the experiments and numerical simulation were perfectly compatible.

REFERENCES

Aizawa, Y., Nishiwaki, J., Harada, Y., Muraishi, S., Kumai, S. (2016). Experimental and numerical analysis of the formation behavior of intermediate layers at explosive welded Al/Fe joint interfaces. *J. Manuf. Process.* 24, 100–106. https://doi.org/10.1016/j.jmapro.2016.08.002.

Akbari Mousavi, S.A.A., Al-Hassani, S.T.S. (2008). Finite element simulation of explosively-driven plate impact with application to explosive welding. *Mater. Design* 29 (1), 1–19. https://doi.org/10.1016/j.matdes.2006.12.012.

Bataev, I.A., Bataev, A.A., Mali, V.I., Pavliukova, D.V. (2012). Structural and mechanical properties of metallic-intermetallic laminate composites produced by explosive welding and annealing. *Mater. Design* 35, 225–334. https://doi.org/10.1016/j.matdes.2011.09.030.

Cowan, G.R., Bergmann, O.R., Holtzman, A.H. (1971). Mechanism of bond zone wave formation in explosion-clad metals. *Metall. Mater. Trans. B.* 2, 3145–3155. https://doi.org/10.1007/BF02814967.

Deribas, A. (1972). *Physics of explosive hardening and welding*. Nauka, Novosibirsk, USSR.

Gülenc, B., Kaya, Y., Durgutlu, A., Gülenc, I.T., Yildirim, M.S., Kahraman, N. (2016). Production of wire reinforced composite materials through explosive welding.

Arch. Civ. Mech. Eng. 16 (1), 1–8. https://doi.org/10.1016/j.acme.2015.09.006.

Honh-bo, X., Shao-gang, W., Hai-feng, B. (2014). Microstructure and mechanical properties of Ti/Al explosive cladding. *Mater. Design* 56, 1014–1019. https://doi.org/10.1016/j.matdes.2013.12.012.

Hoseini-Athar, M.M., Tolaminejad, B. (2015). Weldability window and the effect of interface morphology on the properties of Al/Cu/Al laminated composites fabricated by explosive welding. *Mater. Design* 86, 516–525. https://doi.org/10.1016/j.matdes.2015.07.114.

Huagui, H., Jichao, W., Wenwen, L. (2017). Mechanical properties and reinforced mechanism of the stainless steel wire mesh–reinforced Al-matrix composite plate fabricated by twin-roll casting. Adv. *Mech. Eng.* 9 (6), 1–9. https://doi.org/10.1177/1687814017716639.

Khanzadeh, M.R., Bakhtiari, H., Seyedi, M., Ahmadi, H.R. (2017). Simulation and welding window of three layers explosively bonded AA5083 and AA1050 aluminum alloys to carbon steel. *J. Energ. Mater.* 12 (3), 139–152.

Li, Y., Liu, C., Yu, H., Zhao, F., Wu, Zh. (2017). Numerical simulation of Ti/Al bimetal composite fabricated by explosive welding. *Metals.* 7 (10), 407. https://doi.org/10.3390/met7100407.

Los, I.S., Khorin, A.V., Troshkina, E.G., Guskov, M.S. (2010). Al–Cu composite by explosive welding. *X international symposium on explosive production of new materials: Science, Technology, Business and Innovations (EPNM-2010).* Bechichi, Montenegro, pp.1–14.

Mendes, R., Ribeiro, J.B., Loureiro, A. (2013). Effect of explosive characteristics on the explosive welding of stainless steel to carbon steel in cylindrical configuration. *Mater. Design* 51, 182–192. https://doi.org/10.1016/j.matdes.2013.03.069.

Nassiri, A., Chini, G.P., Kinsey, B.L. (2015a). Arbitrary lagrangian Eulerian FEA method to predict wavy pattern and weldability window during magnetic pulsed welding. Proceedings of the ASME 2015 Inter. *MSEC2015-9442,* pp. 8–12. https://doi.org/10.1115/MSEC2015-9442.

Nassiri, A., Chini, G., Vivek, A., Daehn, G., Kinsey, B. (2015b). Arbitrary Lagrangian-Eulerian finite element simulation and experimental investigation of wavy interfacial morphology during high velocity impact welding. *Mater. Design* 88, 345–358. https://doi.org/10.1016/j.matdes.2015.09.005.

Patterson, R. (1993). *Fundamentals of explosion welding. ASM Handbook*, pp. 60–164.

Pronichev, D.V., Gurevich, L.M., Trykov, Y.P., Trunov, M.D. (2016). Investigation on contact melting of Cu/Al laminated composite. *Rev. Metal.* 52 (4), e079. https://doi.org/10.3989/revmetalm.079.

Ribeiro, J.B., Mendes, R., Loureiro, A. (2014). Review of the weldability window concept and equation for explosive welding. *J. Phys.: Conf. Ser.* 500 (5), 052038. https://doi.org/10.1088/1742-6596/500/5/052038.

Roudbari, M., Mehdipoor, A., Azarafza, R. (2013). Heat treatment of stainless steel 316L- titanium bimetal manufactured by explosive welding. *IRJABS* 7 (10), 687–692. http://www.irjabs.com/files_site/paperlist/r_2003_140406222643.pdf.

Song, J., Raabe, D., Eggeler, G. (2011). Microstructure and properties of interfaces formed by explosion cladding of titanium to low carbon steel. Ph.D. Thesis, Ruhr-University Bochum, Germany.

Wittman, R. (1973). The influence of collision parameters on the strength and microstructure of an explosion welded aluminum alloy. Proceedings of 2nd Symposium on Use of Explosive Energy in Manufacturing Metallic Materials of New Properties and Possibilities of Application thereof in the Chemical Industry, pp. 153–168.

Xunzhong, G., Jie, T., Wentao, W., Huaguan, L., Chen, W. (2013). Effects of the inner mould material on the aluminium-316L stainless steel explosive clad pipe. *Mater. Design* 49, 116– 122. https://doi.org/10.1016/j.matdes.2013.02.001.

Yingbin, L., Chao, L., Xiaoyan, H., Chufan, Y., Tiansheng, L. (2017). Explosive welding of copper to high nitrogen austenitic stainless steel. *Metals* 9 (3), 339. https://doi.org/10.3390/met9030339.

Zakharenko, I., Zlobin, B. (1983). Effect of the hardness of welded materials on the position of the lower limit of explosive welding combust. *Combust. Explos. Shock Waves* 19, 689–692. https://doi.org/10.1007/BF00750461.

Zamani, E., Lighat, G.H. (2012). Explosive welding of Stainless Steel-Carbon steel coaxial pipes. *J. Mater. Sci*. 47, 685–695. https://doi.org/10.1007/s10853-011-5841-9.